Can J Diabetes 43 (2019) 165–172

Contents lists available at ScienceDirect

Canadian Journal of Diabetes

journal homepage: www.canadianjournalofdiabetes.com

Original Research

Celastrol Reverses Palmitic Acid-Induced Insulin Resistance in HepG2 Cells via Restoring the miR-223 and GLUT4 Pathway

Xue Zhang MM [a,1]; Xiao-Cheng Xue MM [b,1]; Ying Wang PhD [a]; Fan-Fan Cao MM [a]; Jun You BM [a]; Georges Uzan PhD [c]; Bin Peng MD [a,1]; Deng-Hai Zhang MD, PhD [a,c,*,1]

[a] *Sino-French Cooperative Central Lab, Shanghai Gongli Hospital, The Secondary Military Medical University, Shanghai, China*
[b] *Department of Otolaryngology, Shanghai Gongli Hospital, The Secondary Military Medical University, Shanghai, China*
[c] *Inserm, Lavoisier Building, Paul Brousse Hospital, Villejuif, France*

Key Messages

- Celastrol reversed palmitic acid-induced insulin resistance.
- Celastrol attenuated palmitic acid-induced insulin resistance-related alterations in GLUT4 and IRS-1.
- Palmitic acid caused alterations in 9 microRNAs reportedly related to insulin sensitivity, 6 of which were reversed by celastrol.
- MiR-223 is crucial to celastrol's anti-insulin resistance effects.

ARTICLE INFO

Article history:
Received 23 October 2017
Received in revised form
27 May 2018
Accepted 12 July 2018

Keywords:
celastrol
glucose transporter 4 (GLUT4)
insulin resistance
microRNA-223
palmitic acid

ABSTRACT

Objectives: The natural triterpenoid compound celastrol ameliorates insulin resistance (IR) in animal models, but the underlying molecular mechanism is unclear. In this study, we investigated how celastrol regulates IR.
Methods: The HepG2 cellular IR model was initially established with palmitic acid (PA). The expression and activity of glucose transporter 4 (GLUT4), insulin receptor substrate-1 (IRS1) and 9 microRNAs (miRNAs) (miR-7, -34a, -96, -113, -126, -145, -150, -223 and -370) were detected before and after celastrol treatment using the PA-induced HepG2 IR model.
Results: The results showed that 250 μM PA for ≥2 days was optimal for inducing IR in HepG2 cells; 600 nM celastrol significantly attenuated the PA-induced IR in HepG2 cells. The PA-induced GLUT4 and IRS1 downregulation and Ser307 phosphorylation on IRS1 was reversed by subsequent treatment with 600 nM celastrol for 6 h. We next investigated which IR-related miRNAs were possible upstream regulators of celastrol-mediated reversal of PA-induced HepG2 IR. Two miRNAs, miR-150 and -223, were significantly downregulated by PA and were re-raised by subsequent celastrol treatment; and miR-223 was upstream of miR-150. Moreover, knocking down miR-223 abolished celastrol's anti-IR effects in the PA-induced model.
Conclusions: Collectively, our results demonstrated that celastrol reverses PA-induced IR-related alterations, in part via miR-223 in HepG2 cells. Further investigation is warranted for establishing the clinical potential of celastrol in treating IR-related disorders.

RÉSUMÉ

Objectifs : Le célastrol, un composé triterpénoïde naturel, améliore la résistance à l'insuline (RI) chez les modèles animaux, mais on ignore le mécanisme moléculaire sous-jacent. Dans la présente étude, nous avons cherché à savoir comment le célastrol régule la RI.

Mots clés :
célastrol
transporteur de glucose 4 (GLUT4)
résistance à l'insuline
miARN-223
acide palmitique

* Address for correspondence: Deng-Hai Zhang, MD, PhD, Sino-French Cooperative Central Lab, Shanghai Gongli Hospital, The Secondary Military Medical University, 207 Ju Ye Road, Pudong New District, Shanghai 200135, China.
E-mail address: denghai_zhang@163.com
[1]These authors contributed equally to the work.

1499-2671 © 2019 Canadian Diabetes Association.
The Canadian Diabetes Association is the registered owner of the name Diabetes Canada.
https://doi.org/10.1016/j.jcjd.2018.07.002

Méthodes : Le modèle cellulaire HepG2 de RI a initialement été établi par l'acide palmitique (AP). Nous avons détecté l'expression et l'activité du transporteur de glucose 4 (GLUT4), du substrat 1 du récepteur de l'insuline 1 (IRS1) et de 9 microARN (miARN) (miR-7, -34a, -96, -113, -126, -145, -150, -223 et -370) avant et après le traitement par célastrol à l'aide du modèle HepG2 de RI induite par l'AP.
Résultats : Les résultats ont montré qu'une dose de 250 µM d'AP durant 2 jours était optimale pour réduire la RI dans les cellules HepG2et qu'une dose de 600 nM de célastrol atténuait de manière significative la RI induite par l'AP dans les cellules HepG2. La régulation à la baisse du GLUT4 et de l'IRS1 induite par l'AP et la phosphorylation de la Ser307 sur l'IRS1 était annulée par le traitement subséquent par 600 nM de célastrol durant 6 h. Nous avons ensuite examiné les miARN liés à la RI pour savoir lesquels étaient des régulateurs possibles en amont de la suppression médiée par le célastrol de la RI des HepG2 induite par l'AP. Deux miARN, miR-150 et miR-223, ont montré une régulation significative à la baisse par l'AP et ont montré une réaugmentation après le traitement par célastrol, et le miR-223 était en amont du miR-150. De plus, le *knock-down* du miR-223 supprimait les effets anti-RI du célastrol dans le modèle induit par l'AP.
Conclusions : Ensemble, nos résultats ont démontré que le célastrol annulait les modifications liées à la RI induite par l'AP, en partie par l'intermédiaire du miR-223 dans les cellules HepG2. D'autres études sont justifiées pour établir le potentiel clinique du célastrol dans le traitement des troubles liés à la RI.

Introduction

Insulin resistance (IR) is involved in adipose disorders, diabetes and other metabolic diseases. IR greatly affects an individual's quality of life and is becoming a major global health problem (1–3). Thus, there is a need to discover a new and effective anti-IR drug that has minimal side effects.

Celastrol is a triterpenoid compound that was first extracted from herbal *Tripterygium wilfordii* Hook F and has been used to treat rheumatic diseases in China for many years (4). Our research team, as well as others, have shown that celastrol can be used as an anti-inflammatory and antitumor agent as well as to ameliorate degenerative neural diseases (5–9). More recently, celastrol was found to improve IR. Yu et al (2009) reported that celastrol improved insulin sensitivity in fructose-induced hypertension in rats (10). Kim et al (2012) found that celastrol administered for 2 months in db/db mice significantly lowered fasting plasma glucose, glycated hemoglobin (A1C) and homeostasis model assessment index levels (11). Both studies proposed that celastrol's therapeutic effects were mediated by its antioxidant and anti-inflammatory properties. Indeed, these properties were also demonstrated in other models (4). However, IR, which might be caused by various pathologic factors, is ultimately related to changes in insulin-signaling pathways (2). Stimulation of the insulin receptor by factors that activate insulin receptor substrate-1 (IRS1) to induce glucose transporter (GLUT) translocation has been studied intensively (12). However, it remains unclear whether celastrol can restore IR-related abnormal insulin signaling.

Hunnicutt et al reported that long-term treatment with palmitic acid (PA) can cause IR (13). PA-induced cells have been widely used as an IR model in vitro and have shown that typical molecular alterations, such as IRS1 phosphorylation and GLUT-level alteration, play roles in IR (14). In this study, we investigated the effects of celastrol on IR-related alterations in the PA-induced HepG2 cellular IR model. MicroRNAs (miRs) are important regulators of insulin pathways and can contribute to IR (15,16). Therefore, to further understand the detailed mechanism of celastrol in attenuating IR, we explored the effects of celastrol on a panel of miRs that have been reported to regulate GLUTs and IRS1s (17–25).

Methods

Reagents and chemicals

Fetal bovine serum, minimum essential medium (MEM) and streptomycin/penicillin were purchased from PAA Laboratories (Linz, Austria). Bovine serum albumin was obtained from Equitech-Bio (Kerrville, Texas, United States). Dimethyl sulfoxide (DMSO), PA and celastrol came from Sigma (St. Louis, Missouri, United States). Anti-IRS1 antibody came from Epitomics (Burlingame, California, United States). Anti-GLUT4 and anti-IRS1 (Ser307) came from Sigma. The BCA protein assay reagent kit, antiactin antibody, protein extraction lysis buffer and Beyo Enhanced Chemiluminescence Plus came from Beyotime Biotechnology (Jiangsu, China). A total RNA extraction kit was purchased from Shanghai Fastagen Biotechnology (Shanghai, China). Rever Tra Ace Q-PCR RT Master Mix and Realtime PCR Master Mix were purchased from Toyobo (Osaka, Japan). miRNA-specific reverse transcription primers and real-time kit, anti-miRNA antagomir for downregulation and miRNA mimetic for overexpression of miR-150 or miR-223 and their controls and siRNA-MATE were purchased from GenePharma (Shanghai, China).

PA and celastrol stock solution preparation

According to the method of Cousin et al (26), 100 mmol/L PA stock solution was prepared in 0.1 mol/L NaOH. The PA stock solution is stable for 1 to 2 weeks at –20°C or for 3 to 4 weeks at –80°C.

Then, 50 mmol/L celastrol was dissolved in DMSO, stored at –20°C and used within 3 months after preparation. The stock solution was then diluted with Roswell Park Memorial Institute (RPMI) 1640 medium to obtain a working concentration immediately before the cellular proliferation assay.

Cell culture, PA and celastrol treatment

Human hepatocellular carcinoma cell line HepG2 cells purchased from the Shanghai Cell Bank of the National Science Academy of China (Shanghai, China) were cultured in complete MEM medium (10% FBS with 100 IU/mL penicillin and 100 µg/mL streptomycin) in a 37°C incubator with humidified 5% CO_2. Cells were seeded in complete MEM medium in culture flasks overnight, and the medium was replaced with fresh complete MEM containing 100 µmol/L PA. After 2 days, the medium was replaced by fresh complete MEM containing 250 µmol/L PA for another 2 days or 28 days. The cells cultured with 0.2% BSA (vehicle) MEM medium served as the PA control. The PA-induced cells were seeded in 6-well culture plates at 1.5×10^6 cells per well overnight. Celastrol was added into the culture medium to reach a final concentration of 600 nmol/L for 6 h. The cells treated with DMSO (same volume of celastrol)-containing culture medium served as the controls. Each test was repeated at least 3 times.

Cell viability assay

Cell viability was assessed by a 3-(4,5-dimethylthiazol-2-yl)-2, 5-diphenyl-tetrazolium bromide (MTT) assay. We seeded 10,000 cells per well in a 96-well flat-bottomed plate for 24 h; then various concentrations of celastrol in medium were added. The cells treated with DMSO (same volume of celastrol)-containing culture medium served as the control. At 6 h after incubation, the MTT solution (5 mg/mL, 20 μL) was added to each well. The relative number of surviving cells was assessed by measuring the optical density of cell lysates at 560 nm. All assays were performed in triplicate wells and repeated at least 3 times.

Glucose uptake measurement

Following the various treatments, the cells were washed with PBS, and 200 μL of 50 μM 2-(N-(7-nitrobenz-2-oxa-1,3-diazol-4-yl)amino)-2-deoxyglucose (2-NBDG)-containing PBS, with or without insulin at the indicated concentrations, was added to the cells. The cells were then kept at 37°C in the dark for 15 min before flow cytometric (FL) detection. The FL1 detector was applied to detect 2-NBDG intensity, and BD CellQuest software (Becton, Dickinson, Franklin Lakes, New Jersey, United States) was used to analyze the results.

Extracellular glucose determination

After various treatments, the cells were washed with PBS, and red phenol-free and serum-free DMEM medium containing 1 mM glucose was added, with or without insulin, at the indicated concentrations. After another 12 h of incubation, the medium was collected. The glucose concentration was determined by the glucose oxidase method, using a glucose assay kit (Nanjing Jiancheng Bioengineering Institute, Nanjing, China) according to the manufacturer's protocols. The glucose level at the starting point of the culture was set as 1, and levels following culture conditions were measured proportional to the starting point.

Western blot

The harvested cells were lysed for 30 min at 4°C and centrifuged at 13,000×*g* for 20 min, and the supernatant was used for analysis. Protein concentrations were detected using a BCA protein assay kit (Thermo Fisher Scientific, Waltham, Massachusetts, United States). Then, 40 μg total protein of each sample was loaded on a sodium dodecyl sulphate-polyacrylamide gel electrophoresis (SDS-PAGE) gel, transferred to a nitrocellulose membrane and probed with corresponding antibodies at the manufacturer's recommended concentrations. After reaction with horseradish peroxidase-conjugated secondary antibody, the probed bands were detected by an enhanced chemiluminescence system. The target bands were scanned by G-BOX iChemi XR and quantified by GeneTools software (Syngene, Cambridge, United Kingdom).

Quantitative real-time polymerase chain reaction

Cellular total RNA was isolated using a total RNA extraction kit (Fasagen Biotechnology, Shanghai, China), following the manufacturer's instructions. A single μg of total RNA was reverse-transcribed by the ReverTra Ace qPCR-RT Master Mix kit (Toyobo, Osaka, Japan) with reverse-transcription primers specific for targeting miRNA. The miRNA-specific cDNA was then amplified with Real-time PCR Master Mix (Gene Pharma, Shanghai, China). U6 small nuclear RNA was employed as an endogenous control. All assays were performed in triplicate. Expression levels were defined as fold change relative to the corresponding controls.

Cell transfection

We seeded 1 million HepG2 cells in 6-well plates for 1 day before transfection. The GLUT4 gene, miRNA-down antagomir, miRNA mimetic, siRNA or their controls were transfected into the cells by siRNA-MATE according to the manufacturer's instructions. (All transfection reagents came from GenePharma, Shanghai, China.)

Statistical analysis

Data are shown as mean ± standard error (SE). Statistical comparisons of the samples with differing treatments were analyzed by the matched t test and repeated at least 3 times. $p<0.05$ was considered statistically significant, and $p<0.01$ was considered very significant.

Results

Cellular toxicity of celastrol or PA

Cellular toxicity of celastrol and PA on HepG2 cells was detected using the cellular survival assay method. We found that 600 nM celastrol administered for 24 h was the maximal dose to maintain HepG2 cell survival (Figure 1A) ($p>0.05$ compared to nontreated cells). The maximal dose for HepG2 cell survival was 250 μM PA (Figure 1B) ($p>0.05$ compared to nontreated cells). In addition, 250 μM PA treatment resulted in significantly higher extracellular glucose ($p<0.05$ compared to nontreated cells) in either the absence or the presence of insulin compared to 100 μM PA stimulation ($p>0.05$) in HepG2 cells (Figure 1C), indicating that this concentration impairs insulin drive and glucose control. Therefore, we applied 250 μM PA to establish a HepG2 cellular IR model in the following experiments and 600 nM celastrol for further detection.

Anti-IR activity of celastrol in the PA-induced HepG2 IR model

Glucose concentration in the culture medium in the cells treated with 250 μM PA or PA+DMSO remained at a higher level with or without 100 nM insulin stimulation for 48 h compared to the untreated cells ($p<0.05$), indicating that PA impairs the ability to balance cellular glucose. However, coincubating cells with 600 nM celastrol for the last 6 h of the 48-h PA treatment successfully restored the cellular balance (reduced) of the glucose level in the culture medium ($p<0.05$) (Figure 1D). Accordingly, 250 μM of PA decreased 15-min cellular glucose-uptake, regardless of insulin stimulation. Again, our data indicate that coincubation with celastrol can correct PA-induced abnormalities (Figure 1E).

Celastrol reversed PA-caused IR-related alterations in GLUT4 and IRS1; re-raising the GLUT4 level was crucial for celastrol to correct PA-induced IR in HepG2

To further explore celastrol's mechanism, we investigated potential alterations of several IR-regulating molecules. After 2 days of incubation with 250 μM PA, GLUT4 and IRS1 protein expression were significantly decreased ($p<0.05$), while phosphorylation of Ser307 on IRS1 was increased ($p<0.05$) (Figure 2A). These alterations suggest that the cells were in an IR state (11). Notably, celastrol treatment for 6 h reversed these alterations ($p<0.05$) (Figure 2A). It is worth noting that the cells did not adapt to long-term PA treatment (28 days). However, alterations in GLUT4 and IRS1, as well as IRS1 phosphorylation, were significantly reversed by 6-h celastrol treatment after 28 days of PA administration (Figure 2B).

To verify the crucial role of GLUT4 in IR signaling, we knocked down GLUT4 protein expression with the corresponding siRNA.

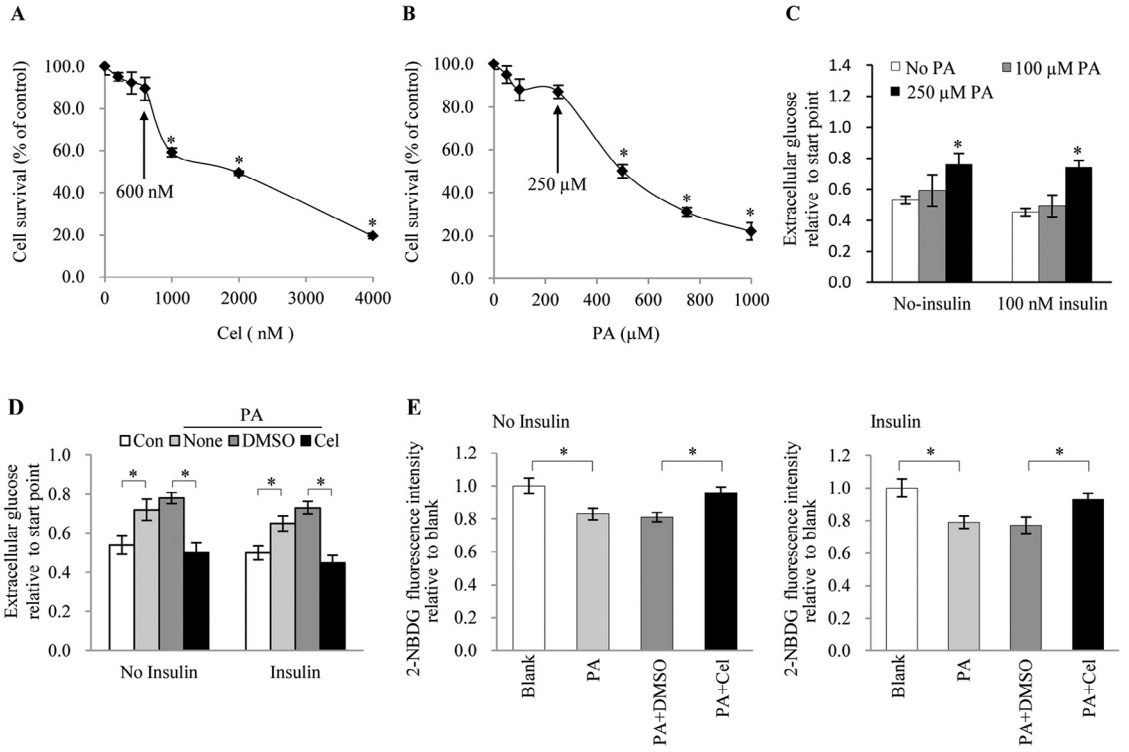

Figure 1. Effects of PA or PA plus celastrol on cellular insulin sensitivity. HepG2 cells were incubated with the indicated dose of celastrol for 1 day (A) or PA for 2 days (B). The survival rates of HepG2 cells were quantified by MTT. HepG2 cells were treated with 100 or 250 μM PA for 2 days, then deprived of glucose for 6 h, After this basic treatment, the cells were cultured in serum-free and red phenol-free medium containing 1 nM glucose with or without 100 nM insulin for 12 h before glucose in the medium was determined by the glucose oxidase method (C). Cells were treated (or not) with PA (250 μM) for 2 days, and for the last 6 h of incubation, celastrol (600 nM), DMSO or neither was loaded with PA-treated cells. Cells in the various groups were then deprived of glucose for 6 h. After these pretreatments, the cells were used to determine the abilities to lower glucose in medium (D), using the methods mentioned in (C). After pretreatments, as mentioned in (C), the cells were incubated with 2-NBDG (a fluorescent glucose analog)-labeled glucose for 15 min; then, the cellular fluorescent intensities were determined via flow cytometry (E). All data are presented as mean ± SE; the sample size (n) for each group is at least 3. *p<0.05; **p<0.01, as compared to untreated control or paired comparisons, as indicated. *Con,* untreated control; *Cel,* celastrol; *MTT,* 3-(4,5-dimethylthiazol-2-yl)-2, 5-diphenyl-trtrazolium bromide; *PA,* palmitic acid.

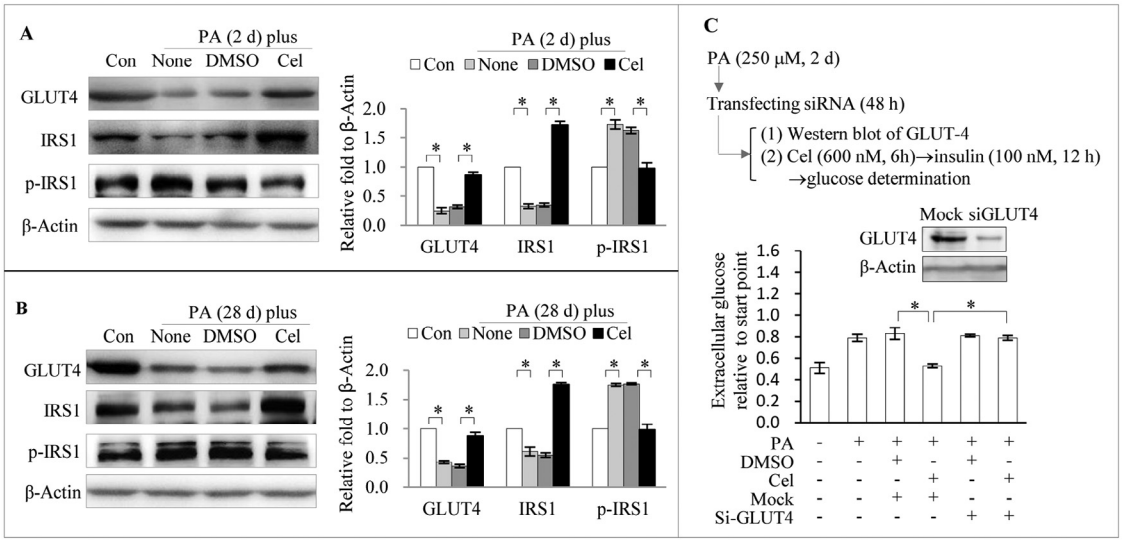

Figure 2. Celastrol attenuates PA-induced GLUT4 and IRS1 depression and IRS1 phosphorylation in a PA-induced HepG2 cellular IR model. GLUT4 silencing decreases the preventive activity of celastrol on PA-induced HepG2 IR. HepG2 cells were incubated with 250 μM PA for 2 days (A) or 28 days (B) and then treated with or without 600 nM celastrol for 6 h. GLUT4 and IRS-1 protein expression and IRS1 phosphorylation at Ser307 were detected by Western blot. Extracellular glucose levels were determined using a glucose oxidase method in the cells treated with nothing (None), PA, DMSO, celastrol, GLUT4-siRNA-silence (siGLUT4)+DMSO, or GLUT4-siRNA-silence+celastrol, respectively. The representative images show effective activity of GLUT4 siRNA. Statistical data are presented as mean ± SE; the sample size (n) for each group is at least 3. *p<0.05; **p<0.01 when compared as indicated, or between the treated groups and untreated control. *Con,* control; *Cel,* celastrol; *PA,* palmitic acid; *p-IRS1,* ser307 phosphorylation on IRS-1; *siGLUT4,* cells transfected with siRNA for GLUT4.

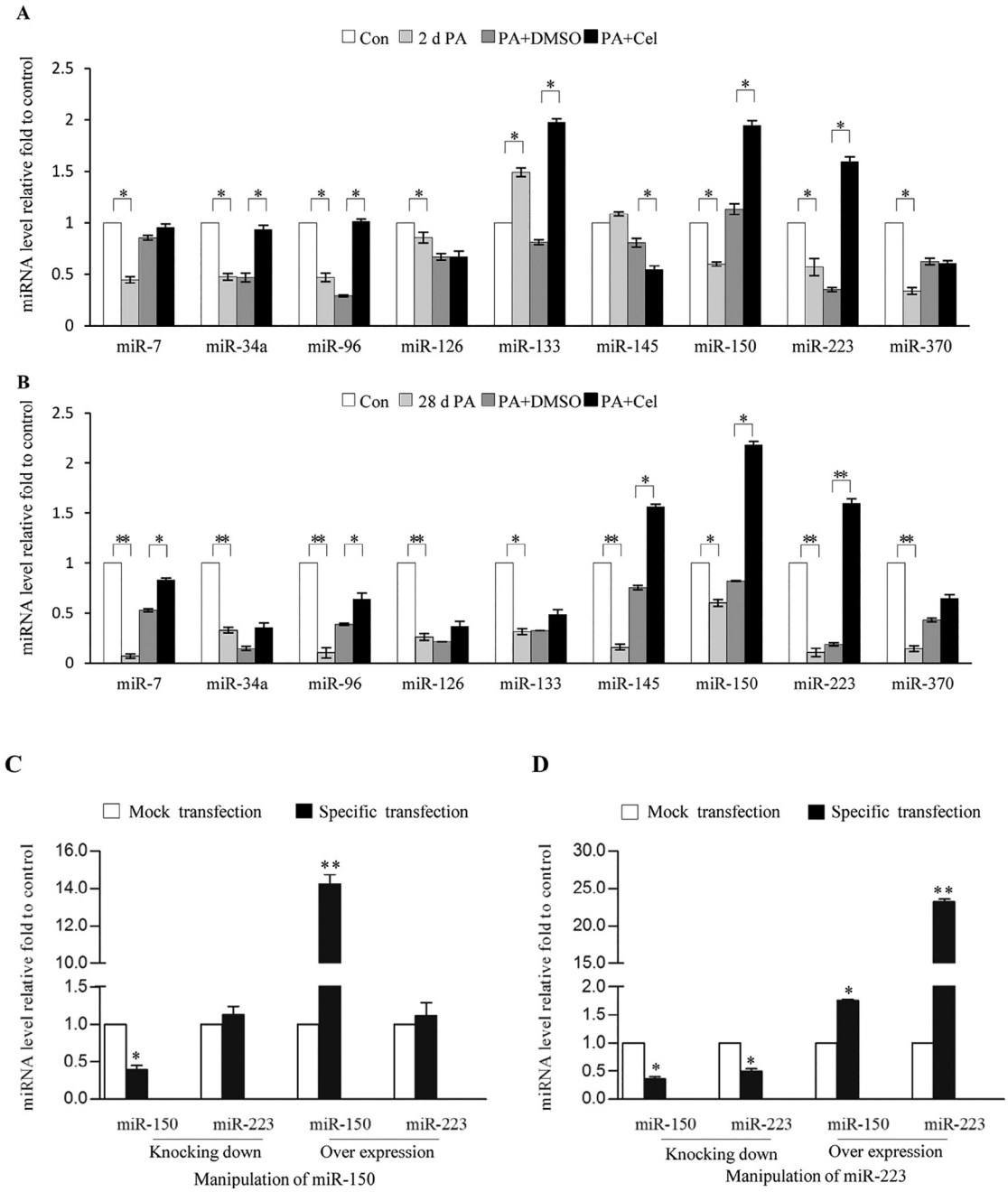

Figure 3. IR-related miRNA levels following celastrol treatment of PA-induced HepG2 cells. HepG2 cells were pretreated with PA at a final concentration of 250 μM for 2 days (A) or 28 days (B) and then stimulated or not with 600 nM celastrol for 6 h. The indicated miRNAs were quantified by Q-PCR. HepG2 cells were transfected with miR-150 or -223 mimetics or miR-150 or -223 antagomirs for 48 h (C). MiR-150 and miR-223 levels were quantified by Q-PCR. *p<0.05; **p<0.01; ***p<0.001. The sample size for each group was 3. *Cel*, celastrol; *Con*, control; *IR*, insulin resistance; *PA*, palmitic acid.; *Q-PRC*, quantitative polymerase chain reaction.

GLUT4 siRNA clearly reduced celastrol's insulin-driven glucose-lowering ability in the PA-treated cells (Figure 2C).

Celastrol reverses PA-induced alterations of insulin-activated miRNAs

MiRNAs are endogenous RNA silencers that regulate protein expression at the post-transcription level (27). Others have shown that a group of miRNAs are involved in IR regulation (15,16) through controlling insulin activity (18,20,22,25,28). To investigate the possible molecular mechanism of the anti-IR activity of celastrol, we examined the expressions of 9 miRNAs that were reportedly related to IR (17–25) in the PA-induced HepG2 IR system, with or without 600 nM celastrol, for 6 h. The results showed that after PA induction, expression of miR-7, -34a, -96, -150, -223 and -370 were significantly decreased ($p<0.05$), while miR-133 was significantly increased ($p<0.05$) when compared to the negative control cells. The levels of miR-126 and -145 were not significantly altered in the PA-induced group (Figure 3A). Interestingly, celastrol treatment significantly reversed the PA-induced decrease of miR-34a, -96, -150 and -223 compared to the DMSO control cells. Notably, expression of miR-150 and -223 were significantly upregulated compared to normal HepG2 cells. The miR-34a and -96 levels were restored to normal levels (Figure 3A). Celastrol treatment further increased the miR-133 level in PA pretreated HepG2 cells. The PA-decreased miR-7 and miR-370 levels were returned to normal

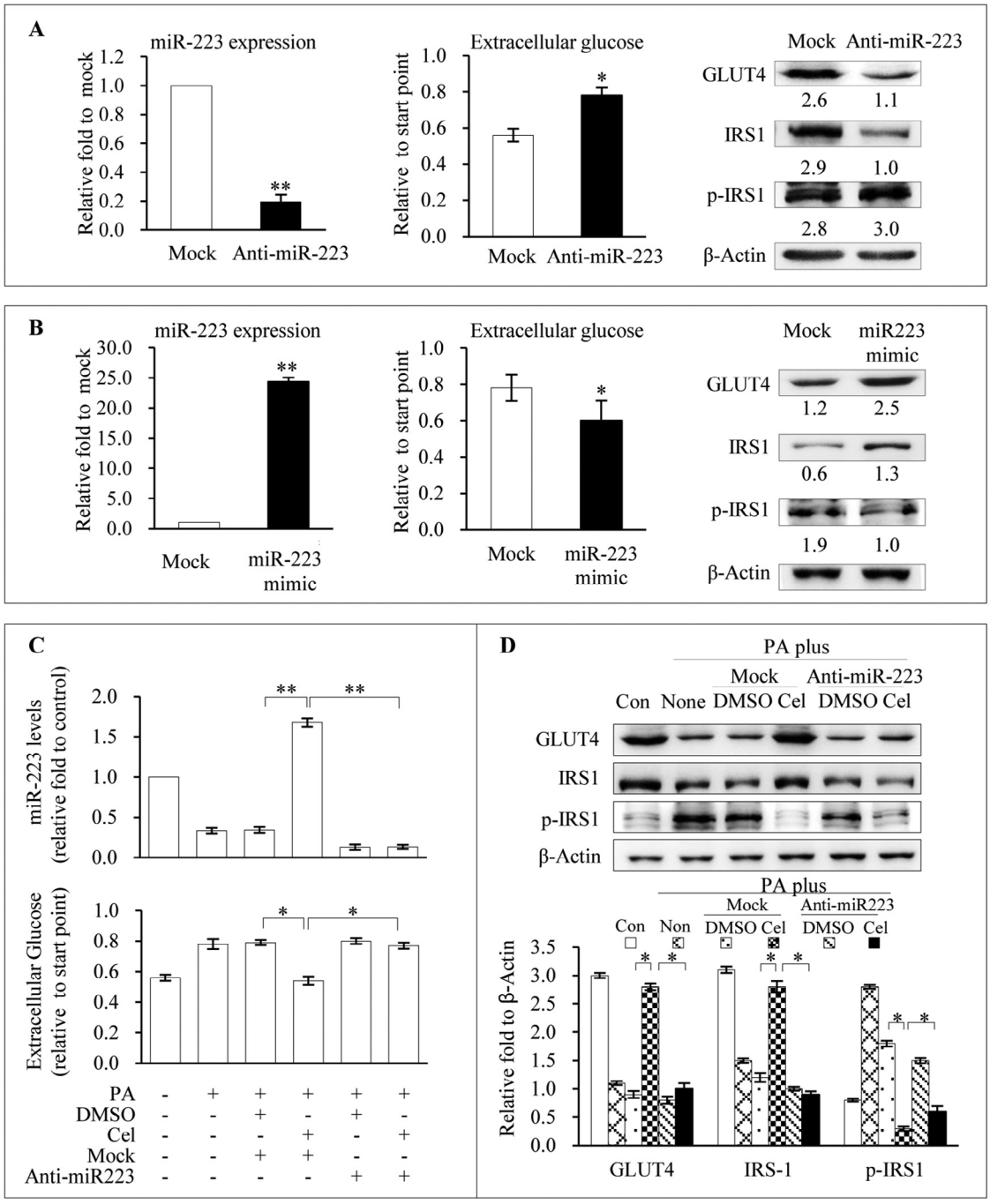

Figure 4. The role of miR-223 in celastrol-mediated anti-IR signaling. HepG2 cells were transfected with miRNA-223 antagomir for 2 days to downregulate miR-223 (A). Nonspecific transfection (mock) was used as the control. Cellular miR-223 expression, glucose levels in the culture medium, and GLUT4 and IRS1 protein expression were detected (B). HepG2 cells were transfected with miR-223 mimetics for 2 days to upregulate miR-223. Nonspecific transfection (mock) was used as the control. Cellular miR-223 expression, glucose levels in the culture medium, and GLUT4 and IRS1 protein expression were detected (C). The glucose levels were analyzed in the miRNA223 antagomir-transfected HepG2 cells (as in A) treated with DMSO or celastrol. Cells treated with nothing (non), PA, DMSO or celastrol were used as the controls (D). GLUT4 and IRS1 expression were examined in the miRNA223 antagomir-transfected HepG2 cells (as in A) treated with DMSO or celastrol. Cells treated with nothing (non), PA, DMSO or celastrol were used as the controls. Data are presented as mean ± SE; the sample size (n) for each group was at least 3. *p<0.05; **p<0.01, as compared to the untreated control or paired comparisons, as indicated. *Con,* untreated control; *Cel*, celastrol; *IR,* insulin resistance; *PA,* palmitic acid.

levels by celastrol. These alterations were similar to those of the DMSO treatment. Therefore, upregulation of miR-7 and miR-370 were attributed to DMSO's effect. DMSO also slightly affected miR-150 expression (Figure 3A).

In contrast to the cells treated with PA for 2 days, all 9 miRNAs were decreased in the cells treated for 28 days. In addition, miR-7, -34a, -96, -150 and -223 expression was severely reduced at 28 days compared to the 2-day-treated cells (Figure 4B). Celastrol significantly elevated miRNA-145, -150 and -223 and restored the miR-7 to normal levels, partially restoring miR-34a, -96, -126 and -133 levels after 28 days of PA (Figure 3B).

Among the 9 miRNAs investigated, miR-150 and miR-223 showed consistent patterns at both 2 days and 28 days of PA treatment; the altered patterns were similar to GLUT4, IRS1 and IRS1 Ser307

phosphorylation patterns. We therefore investigated any mutual effects of these 2 miRNAs. Notably, overexpressing or knocking down miR-150 did not affect miR-223 levels (Figure 3C); yet, overexpressing and knocking down miR-223 increased and decreased miR-150 levels, respectively (Figure 3C). Thus, miR-223 is likely an upstream regulator of miR-150 and, thus, important in our IR model.

miR-223 is a crucial factor involved in celastrol's anti-IR signaling

Next, we investigated the regulatory mechanism of miR-223 on celastrol's anti-PA-induced IR. MiR-223 downregulation reduced the glucose-lowering ability and GLUT4 and IRS1 expression, compared to nonspecific transfection (Figure 4A). In contrast, miR-223 overexpression prevented a subsequent PA-induced glucose increase and GLUT4 and IRS1 downregulation compared to the nonspecific transfection (Figure 4B). Strikingly, miR-223 downregulation abolished celastrol's anti-IR activity in the PA-induced IR HepG2 cell model, resulting in increased glucose levels and downregulated GLUT4 and IRS1 expression (Figure 4C and 4D). These results indicate that miR-223 is a crucial factor in celastrol's anti-IR signaling.

Discussion

The goal of this study was to investigate the mechanism by which celastrol ameliorates IR. Specifically, we explored the effects of celastrol on PA-induced IR-related alterations. The results indicated that celastrol can reverse PA-induced decreases in GLUT4 and IRS1 expression, as well as hyperphosphorylation of IRS1 at Ser307 in HepG2 cells. Celastrol's actions were further verified to be mediated through miR-223 upregulation, the manipulation of which could interfere with GLUT4, IRS1 expression as well as IRS1 Ser307 phosphorylation.

IR induction by PA was established in the 1990s (13), and since then PA has been widely used to induce IR in various cellular models. Here, we found that 250 μM PA incubation for 2 days in the hepatocyte cell line, HepG2, resulted in IR-related alterations, including decreased expression of GLUT4 and IRS1, as well as hyperphosphorylation of IRS1 at Ser307. These changes persisted in cells administered PA for 28 days. Our results agree with the previous report that incubation of HepG2 cells with 500 μM PA for 24 h reduced expression of IRS1, phosphatidylinositol-3 kinase and p85 protein and enhanced phosphorylated IRS1 at Ser307 (14). It should be noted, however, that GLUT4 was not investigated in the previous study. In the conditions of our experiment, we found that 500 μM PA reduced the cell survival rate. We also provided evidence that the optimal concentration and induction time of PA was 250 μM for 2 days. Nevertheless, our findings, in combination with previous reports, confirm that PA successfully induces IR-related alterations in HepG2 cells.

Celastrol attenuates IR, which has been attributed to celastrol's anti-inflammation and antioxidative properties (10,11). In addition to these suggested mechanisms, the upregulation of GLUT4 and IRS1 by celastrol found in this study should be considered as other important contributing factors in IR amelioration. GLUT4 translocates to the cell membrane to facilitate glucose uptake after insulin stimulation. GLUT4 downregulation could result in IR (12,29). Tissues from IR models and humans with diabetes exhibit defects in IRS-dependent signaling, including altered IRS1 expression and phosphorylation, especially at Ser307 (30). The combination of our results and the findings that celastrol reduces fructose-induced IR in db/db mice (10,11) suggest that celastrol regulates multiple pathways to ameliorate IR.

Recent studies have indicated that miRNAs are highly involved in IR regulation (15,31–33), and many miRNAs, including GLUT4 and IRS1 (17–25), can regulate insulin metabolic activities. In addition, celastrol has been reported to regulate some miRNAs (34,35). Therefore, we further investigated the possible upstream events of celastrol's anti-IR activity. Our results suggest that 2 miRNAs (miR-150 and miR-223) participate in celastrol's anti-IR activity, because expression of both miRNAs was downregulated by PA and restored by celastrol. More interesting, miR-150 overexpression did not interfere with miR-223 levels, whereas miR-223 overexpression increased miR-150 expression (Figure 3C). The effects of miR-223 overexpression were similar to those of celastrol treatment, indicating that miR-223 might be upstream of miR-150 and a downstream regulator of celastrol (Figure 4A, B). In addition, downregulation of miR-223 totally abolished celastrol's anti-IR activity and decreased GLUT4 and IRS1 expression (Figure 4D). Overexpression of miRNA-223 has been reported to increase GLUT4 protein in cardiomyocytes (22). Combined with this study, a total of 21 proteins in humans have been confirmed to be regulated by miR-223. Among them, 6 were verified to be controlled by celastrol, including GLUT4, IRS1, IKK, PS3, IL6 and HSP90B1 (4,36–38). Eleven genes were targeted by miR-150, and 4 (Myb, VEGFA, CXCR4 and FLT3) were reported to be regulated by celastrol (39–42). This study provides further evidence that celastrol affects miR-223 expression.

Conclusions

Celastrol is effective in reversing PA-impaired insulin sensitivity, as well as PA-caused IR-related alterations in GLUT4 and IRS-1; these effects of celastrol are dependent on re-raising PA-decreased miR-223 levels.

Acknowledgments

This work was supported by the following grants: Shanghai Pudong New Area Gongli Hospital Youth Project (GLRq2017-01 for XZ; GLRq2017-05 for XCX; 2015YQNJJ-01 for XCX); National Natural Science Foundation of China (#81102349 for BP and C-XY); Shanghai Excellent Academic Leader in Medicine (#XBR2011054) and Shanghai Traditional Chinese Medicine Content Construction Innovation Project (ZY3-CCCX-3-7001) for D-HZ; the International Science & Technology Cooperation Project of China (Grant 2011DFB30010 for M-QL and GU); Shanghai Municipal Commission of Health and Family Planning Project (#201540394 for B.P); Key disciplines of health systems in Shanghai Pudong New Area (#PWZxq2017-04 for XCX).

Author Disclosures

Conflicts of interest: None.

Author Contributions

XZ carried out the cell culture, participated in the design of the study, performed statistical analysis and drafted the manuscript; XXC carried out cell culture detection; YW participated in cell culture; FC participated in flow cytometry detection; BP participated in the study design and helped to draft the manuscript; DZ conceived of the study, participated in its design and coordination and helped to draft the manuscript. All authors have read and approved the final manuscript.

References

1. Ginter E, Simko V. Type 2 diabetes mellitus, pandemic in 21st century. Adv Exp Med Biol 2012;771:42–50.

2. Johnson AM, Olefsky JM. The origins and drivers of insulin resistance. Cell 2013;152:673–84.
3. Toth PP. Insulin resistance, small LDL particles, and risk for atherosclerotic disease. Curr Vasc Pharmacol 2014;12:653–7.
4. Salminen A, Lehtonen M, Paimela T, Kaarniranta K. Celastrol: Molecular targets of thunder god vine. Biochem Biophys Res Commun 2010;394:439–42.
5. Allison AC, Cacabelos R, Lombardi VR, Alvarez XA, Vigo C. Celastrol, a potent antioxidant and anti-inflammatory drug, as a possible treatment for Alzheimer's disease. Prog Neuropsychopharmacol Biol Psychiatry 2001;25:1341–57.
6. Kannaiyan R, Shanmugam MK, Sethi G. Molecular targets of celastrol derived from thunder of god vine: Potential role in the treatment of inflammatory disorders and cancer. Cancer Lett 2011;303:9–20.
7. Peng B, Xu L, Cao F, et al. HSP90 inhibitor, celastrol, arrests human monocytic leukemia cell U937 at G0/G1 in thiol-containing agents reversible way. Mol Cancer 2010;9:79.
8. Venkatesha SH, Astry B, Nanjundaiah SM, Yu H, Moudgil KD. Suppression of autoimmune arthritis by celastrus-derived celastrol through modulation of proinflammatory chemokines. Bioorg Med Chem 2012;20:5229–34.
9. Zhang DH, Marconi A, Xu LM, et al. Tripterine inhibits the expression of adhesion molecules in activated endothelial cells. J Leukoc Biol 2006;80:309–19.
10. Yu X, Tao W, Jiang F, Li C, Lin J, Liu C. Celastrol attenuates hypertension-induced inflammation and oxidative stress in vascular smooth muscle cells via induction of heme oxygenase-1. Am J Hypertens 2010;23:895–903.
11. Kim JE, Lee MH, Nam DH, et al. Celastrol, an NF-κB inhibitor, improves insulin resistance and attenuates renal injury in db/db mice. PLoS ONE 2013;8:e62068.
12. Bogan JS. Regulation of glucose transporter translocation in health and diabetes. Annu Rev Biochem 2012;81:507–32.
13. Hunnicutt JW, Hardy RW, Williford J, McDonald JM. Saturated fatty acid-induced insulin resistance in rat adipocytes. Diabetes 1994;43:540–5.
14. Lei H, Lu F, Dong H, et al. Genistein reverses free fatty acid-induced insulin resistance in HepG2 hepatocytes through targeting JNK. J Huazhong Univ Sci Technol Med Sci 2011;31:185–9.
15. Fernandez-Valverde SL, Taft RJ, Mattick JS. MicroRNAs in β-cell biology, insulin resistance, diabetes and its complications. Diabetes 2011;60:1825–31.
16. Williams MD, Mitchell GM. MicroRNAs in insulin resistance and obesity. Exp Diabetes Res 2012;2012:484696.
17. Chang KW, Chu TH, Gong NR, et al. miR-370 modulates insulin receptor substrate-1 expression and inhibits the tumor phenotypes of oral carcinoma. Oral Dis 2013;19:611–9.
18. Horie T, Ono K, Nishi H, et al. MicroRNA-133 regulates the expression of GLUT4 by targeting KLF15 and is involved in metabolic control in cardiac myocytes. Biochem Biophys Res Commun 2009;389:315–20.
19. Hua Y, Zhang Y, Ren J. IGF-1 deficiency resists cardiac hypertrophy and myocardial contractile dysfunction: Role of microRNA-1 and microRNA-133a. J Cell Mol Med 2012;16:83–95.
20. Jeong HJ, Park SY, Yang WM, Lee W. The induction of miR-96 by mitochondrial dysfunction causes impaired glycogen synthesis through translational repression of IRS-1 in SK-Hep1 cells. Biochem Biophys Res Commun 2013;434:503–8.
21. La Rocca G, Badin M, Shi B, et al. Mechanism of growth inhibition by MicroRNA 145: The role of the IGF-I receptor signaling pathway. J Cell Physiol 2009;220:485–91.
22. Lu H, Buchan RJ, Cook SA. MicroRNA-223 regulates Glut4 expression and cardiomyocyte glucose metabolism. Cardiovasc Res 2010;86:410–20.
23. Rai K, Takigawa N, Ito S, et al. Liposomal delivery of microRNA-7-expressing plasmid overcomes epidermal growth factor receptor tyrosine kinase inhibitor-resistance in lung cancer cells. Mol Cancer Ther 2011;10:1720–7.
24. Raychaudhuri S. MicroRNAs overexpressed in growth-restricted rat skeletal muscles regulate the glucose transport in cell culture targeting central TGF-β factor SMAD4. PLoS ONE 2012;7:e34596.
25. Zhang J, Du YY, Lin YF, et al. The cell growth suppressor, mir-126, targets IRS-1. Biochem Biophys Res Commun 2008;377:136–40.
26. Cousin SP, Hügl SR, Wrede CE, Kajio H, Myers MG, Rhodes CJ. Free fatty acid-induced inhibition of glucose and insulin-like growth factor I-induced deoxyribonucleic acid synthesis in the pancreatic beta-cell line INS-1. Endocrinology 2001;142:229–40.
27. Ambros V. The functions of animal microRNAs. Nature 2004;431:350–5.
28. Zhang Y, Yang L, Gao YF, et al. MicroRNA-106b induces mitochondrial dysfunction and insulin resistance in C2C12 myotubes by targeting mitofusin-2. Mol Cell Endocrinol 2013;381:230–40.
29. Leto D, Saltiel AR. Regulation of glucose transport by insulin: Traffic control of GLUT4. Nat Rev Mol Cell Biol 2012;13:383–96.
30. Copps KD, White MF. Regulation of insulin sensitivity by serine/threonine phosphorylation of insulin receptor substrate proteins IRS1 and IRS2. Diabetologia 2012;55:2565–82.
31. Gilbert ER, Liu D. Epigenetics: The missing link to understanding β-cell dysfunction in the pathogenesis of type 2 diabetes. Epigenetics 2012;7:841–52.
32. Rottiers V, Näär AM. MicroRNAs in metabolism and metabolic disorders. Nat Rev Mol Cell Biol 2012;13:239–50.
33. Shantikumar S, Caporali A, Emanueli C. Role of microRNAs in diabetes and its cardiovascular complications. Cardiovasc Res 2012;93:583–93.
34. Li H, Li Y, Liu D, Sun H, Liu J. miR-224 is critical for celastrol-induced inhibition of migration and invasion of hepatocellular carcinoma cells. Cell Physiol Biochem 2013;32:448–58.
35. Sha M, Ye J, Zhang LX, Luan ZY, Chen YB. Celastrol induces apoptosis of gastric cancer cells by miR-146a inhibition of NF-κB activity. Cancer Cell Int 2013;13:50.
36. Chadalapaka G, Jutooru I, Safe S. Celastrol decreases specificity proteins (Sp) and fibroblast growth factor receptor-3 (FGFR3) in bladder cancer cells. Carcinogenesis 2012;33:886–94.
37. Kannaiyan R, Hay HS, Rajendran P, et al. Celastrol inhibits proliferation and induces chemosensitization through down-regulation of NF-κB and STAT3 regulated gene products in multiple myeloma cells. Br J Pharmacol 2011;164:1506–21.
38. Lee JH, Koo TH, Yoon H, et al. Inhibition of NF-kappa B activation through targeting I kappa B kinase by celastrol, a quinone methide triterpenoid. Biochem Pharmacol 2006;72:1311–21.
39. Hieronymus H, Lamb J, Ross KN, et al. Gene expression signature-based chemical genomic prediction identifies a novel class of HSP90 pathway modulators. Cancer Cell 2006;10:321–30.
40. Huang L, Zhang Z, Zhang S, et al. Inhibitory action of celastrol on hypoxia-mediated angiogenesis and metastasis via the HIF-1α pathway. Int J Mol Med 2011;27:407–15.
41. Jang SY, Jang SW, Ko J. Celastrol inhibits the growth of estrogen positive human breast cancer cells through modulation of estrogen receptor α. Cancer Lett 2011;300:57–65.
42. Yadav VR, Sung B, Prasad S, et al. Celastrol suppresses invasion of colon and pancreatic cancer cells through the downregulation of expression of CXCR4 chemokine receptor. J Mol Med 2010;88:1243–53.